AD-A267 614

N PAGE

Form Approved
OBM No. 0704-0188

1. Agency Use Only *(Leave blank).*	2. Report Date. March 1993	3. Report Type and Dates Covered. Final - Proceedings

4. Title and Subtitle.
Evaluating ERS-1 Ice Motion and Classification Products

5. Funding Numbers.
Program Element No. 0603704N
Project No. 00101
Task No. 100
Accession No. DN258116
Work Unit No. 572518903

6. Author(s).
F. Fetterer and D. Gineris*

7. Performing Organization Name(s) and Address(es).
Naval Research Laboratory
Remote Sensing Applications Branch
Stennis Space Center, MS 39529-5004

8. Performing Organization Report Number.
NRL/PP/7240--92-0002

9. Sponsoring/Monitoring Agency Name(s) and Address(es).
Space and Naval Warfare Systems Command
Arlington, VA 22202

10. Sponsoring/Monitoring Agency Report Number.
NRL/PP/7240--92-0002

11. Supplementary Notes.
Published in Proceedings of the First ERS-1 Symposium.
*Sverdrup Technology

12a. Distribution/Availability Statement.
Approved for public release; distribution is unlimited.

12b. Distribution Code.

13. Abstract *(Maximum 200 words).*

ERS-1 Synthetic Aperture Radar (SAR) imagery from the Alaska SAR Facility is available to operational ice analysts at the Joint Ice Center. Analyst can use the imagery directly through manual interpretation. One such use would be to provide information on ice conditions for a field expediction. In addition, analysts can run automated algorithms which produce estimates of ice type and ice motion from SAR images. Such automated analysis will become increasingly important if SAR is to be used to improve climatologies of ice characteristics and to improve the performance of dynamic ice models. Here the ice classification and ice motion algorithms developed by the Jet Propulsion Laboratory for ERS-1 SAR imagery are evaluated and results presented.

14. Subject Terms.
Remote sensing, synthetic aperture radar, sea ice

15. Number of Pages. 3

16. Price Code.

17. Security Classification of Report.	18. Security Classification of This Page.	19. Security Classification of Abstract.	20. Limitation of Abstract.
Unclassified	Unclassified	Unclassified	SAR

EVALUATING ERS-1 ICE MOTION AND CLASSIFICATION PRODUCTS

F. Fetterer[1], D. Gineris[2]

[1] Remote Sensing Applications Branch, Naval Research Laboratory DET, Stennis Space Center, MS 39520 [2] Sverdrup Technology, Stennis Space Center, MS

ABSTRACT

ERS-1 Synthetic Aperture Radar (SAR) imagery from the Alaska SAR Facility is available to operational ice analysts at the Joint Ice Center. Analysts can use the imagery directly through manual interpretation. One such use would be to provide information on ice conditions for a field expedition. In addition, analysts can run automated algorithms which produce estimates of ice type and ice motion from SAR images. Such automated analysis will become increasingly important if SAR is to be used to improve climatologies of ice characteristics and to improve the performance of dynamic ice models. Here the ice classification and ice motion algorithms developed by the Jet Propulsion Laboratory for ERS-1 SAR imagery are evaluated and results presented.

Acknowledgment. This work was sponsored by the Chief of Naval Operations under program element 603704N, CDR P. Ranelli, program manager. Contribution NRL/PP/7240-92-0002.

Key words: Sea ice, synthetic aperture radar, operational remote sensing

1. INTRODUCTION

1.1 *Objectives*

Through a cooperative agreement between the European Space Agency, the National Aeronautics and Space Administration, and the National Oceanic and Atmospheric Administration, the Joint Ice Center in the United States has access to ERS-1 data from the Alaska SAR Facility (ASF). We have assembled software tools and a data base of satellite imagery with which to evaluate synthetic aperture radar (SAR) image products and to improve the operational usefulness of imagery and products. Some applications for SAR data, such as using ice deformation fields from SAR to update ice prediction models, require further development before they can be implemented operationally. Others, such as using ice type maps from SAR to improve the accuracy of arctic-wide ice analyses, are ready now.

In general, operational usefulness depends on the timeliness with which a SAR image can be obtained and analyzed for a desired area, the accuracy of the result, and the ease with which the product can be relayed to the user. ASF can process SAR data within 6 hours of the satellite pass using predicted orbital elements when necessary. Imagery requested for operational use is displayed on a SAR workstation consisting of a SUN computer and peripherals. The analyst can create an output product by manually interpreting an image, or can run algorithms to automatically produce an ice type map or ice motion vectors. These algorithms, which were developed by the Jet Propulsion Laboratory (JPL), are identical (at this writing) to those which create products at ASF. Here we assess the accuracy of the ice classification product, and compare the ice motion product with other sources of ice drift information. This work is part of a larger program which has as its objective the more efficient use of SAR data for polar applications.

1.2 *Data Set*

ERS-1 SAR imagery of the Beaufort Sea, Chukchi Sea, East Siberian Sea and Central Arctic from March and early April 1992 was selected. We chose this time period because of the availability of coincident satellite visible, infrared, and passive microwave data, and because of the availability of surface validation from the Beaufort Sea Leadex experiment. Figure 1 shows the coverage of the 5 satellite passes from which sixty 100 km-square images were chosen for the assessment of the classification algorithm. Air temperature analyses from the Fleet Numerical Oceanography Center show temperatures well below freezing for the regions covered by these passes.

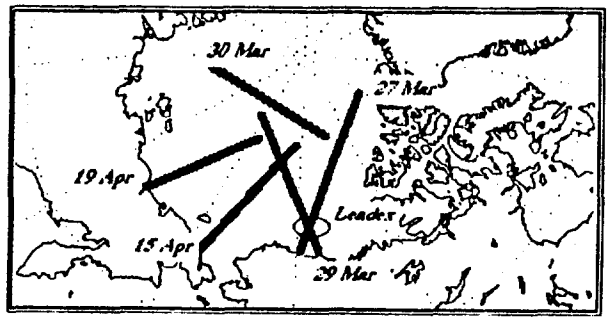

Figure 1. SAR passes selected for evaluation.

2. CLASSIFICATION

2.1 *Algorithm Description*

The ice classification algorithm relies on *a priori* knowledge of backscatter distributions for ice types. Because the algorithm uses low resolution (240 m) multiple look data, the effect of "speckle" or multiplicative noise need not be accommodated. Backscatter measurements obtained by sampling a small portion of a calibrated image are clustered. The cluster with the most members is labeled by referring to a look-up table (LUT) of empirically derived backscatter distributions for multiyear (MY) ice (with mean of -10 dB), two classes of first year (FY) ice (a "dark" FY with backscatter of -17 dB, and "bright" FY with backscatter of -14 dB), and new ice or smooth open water (for the winter algorithm).

The centroid of this cluster is then used for maximum likelihood or minimum distance image pixel classification. The centroids for the other ice types are found simply by using the expected difference between the mean backscatter for these types and the primary type. For a full description, see Ref. 1. The algorithm accommodates a certain amount of variability in the mean backscatter of the dominant type by labeling it according to the LUT type it is closest to, and shifting all other type centroids accordingly. However, natural variability in backscatter for ice types and variability in the difference in mean backscatter between types introduces error.

2.2 *Algorithm Performance*

Classification performance is evaluated by comparing the ice type composition of an image produced by the unsupervised classification algorithm with that produced by supervised classification using training sets. The user has the option of choosing minimum distance or maximum likelihood classification for either supervised or unsupervised classification. Both work equally well for supervised classification, reflecting similarly shaped distributions of FY and MY ice in our data set. Scene classification with maximum likelihood takes about 5 minutes, while minimum distance takes half as long. For unsupervised classification, maximum likelihood performs significantly better in most scenes. The minimum distance classifier noticeably overestimated the percentage of FY ice when MY makes up more than about 80% of the image, because it misclassifies relatively dark pixels within MY floes as FY ice.

Figure 2 shows a comparison of maximum likelihood supervised classification with unsupervised maximum likelihood algorithm classification for MY and FY ice. Each data point is the percentage of MY or FY ice which results from classifying an image using both methods. If supervised classification is regarded as completely accurate, algorithm error can be expressed as the percent difference in concentration given by the two methods (Table 1). Mean difference is probably a good measure of error for MY ice, since the algorithm has a bias toward overestimating MY ice (Fig. 2, top), while the standard deviation of the differences may be a better measure for FY ice, since points are distributed on both sides of the "no error" line (Fig. 2, bottom). If only cases where the percentage of MY is greater than 60% are considered, the error for MY drops to 4% with standard deviation of 4%, while that for FY drops to 4% with standard deviation of 5%. These errors appear random over the time period and range of latitudes covered by the images.

Table 1. Difference in supervised and unsupervised classification concentrations for all images classified.

Surface	Mean	Standard Deviation
MY	8%	12%
Bright FY	8%	10%
Dark FY	8%	14%
All FY	8%	12%

The outlying points in Figure 2 deserve some discussion. FY ice in the fast ice shear zone north of Alaska is classified as MY in 2 scenes because of its bright signature, causing 2 outlying points in Figure 2 (top) with concentration values from supervised classification of about 10%. The same scenes have corresponding outlying points in Figure 2 (bottom). The algorithm's specified domain begins north of this zone. Two outlying points in Figure 2 (top) with concentration values of 0% MY from supervised classification and 60% MY from the algorithm are from scenes at the southern end of the 15 April pass (Fig. 1). FY ice in these scenes has unusually bright mean backscatter of -11.2 dB. A darker FY type in these scenes is -15.0 dB, while MY from scenes further north is -8.9 dB.

2.3 *Backscatter Variability*

Supervised classification provides a measure of the backscatter of the ice samples used for training sets. The mean backscatter values obtained for ice types using 390 samples from 60 images

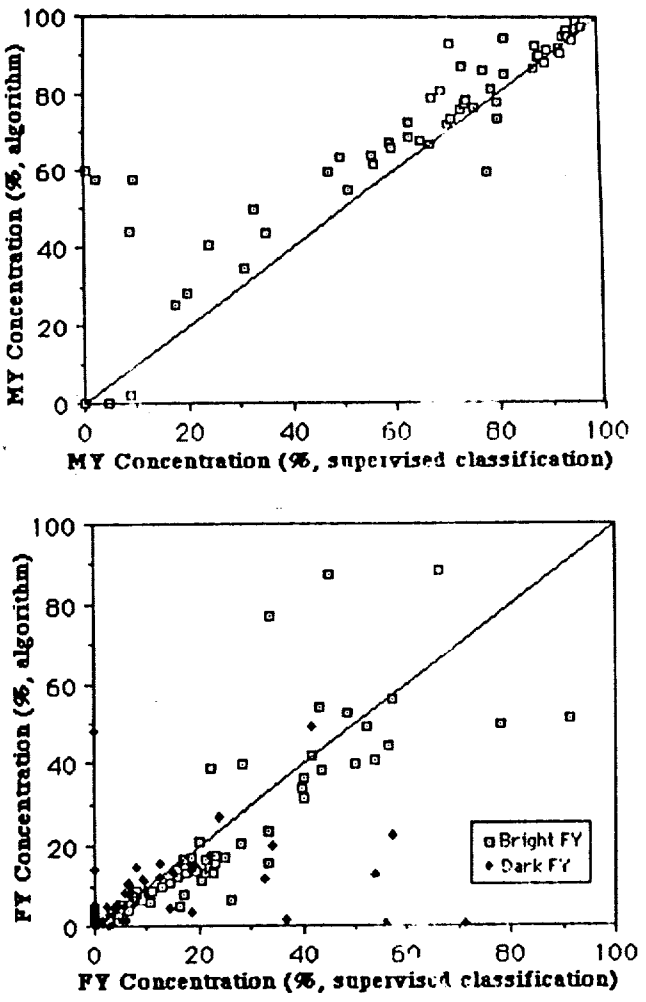

Figure 2. (Top) The concentration of multiyear (MY) ice arrived at through supervised classification versus that produced by the automated algorithm. (Bottom) As above, for first-year (FY) ice.

agreed well (within 0.3 dB for MY and 0.7 dB for FY) with those used by the JPL algorithm. Plots of backscatter versus latitude show interesting variation for both FY and MY ice (Fig. 3). A second-order polynomial is fitted to the data. One unanticipated result of backscatter measurements from a supplementary data set over the Leadex camp was that the backscatter of FY ice in 5 descending passes was, on average, about 1 dB greater than that of the same ice in 5 ascending passes. We ascribe this to scatter from ridges in the FY ice, which appear to be oriented predominantly in the along-track direction for descending passes.

Most scenes in the data set had little or no open water or new ice. While FY and MY ice is reliably classified with a small error, wind-roughened water is classified as MY ice, and the backscatter signature of ice in freezing leads may mimic that of FY or MY ice. In general, however, experience with the classification algorithm showed that it satisfactorily classifies most images in spite of some variability in the mean backscatter of classes from image to image. Variability in the mean backscatter difference between classes from image to image has not been evaluated. Future work involves calculating the theoretical misclassification by the algorithm given the measured backscatter distributions, and evaluating seasonal and regional variation in backscatter from ice and its effect on algorithm performance.

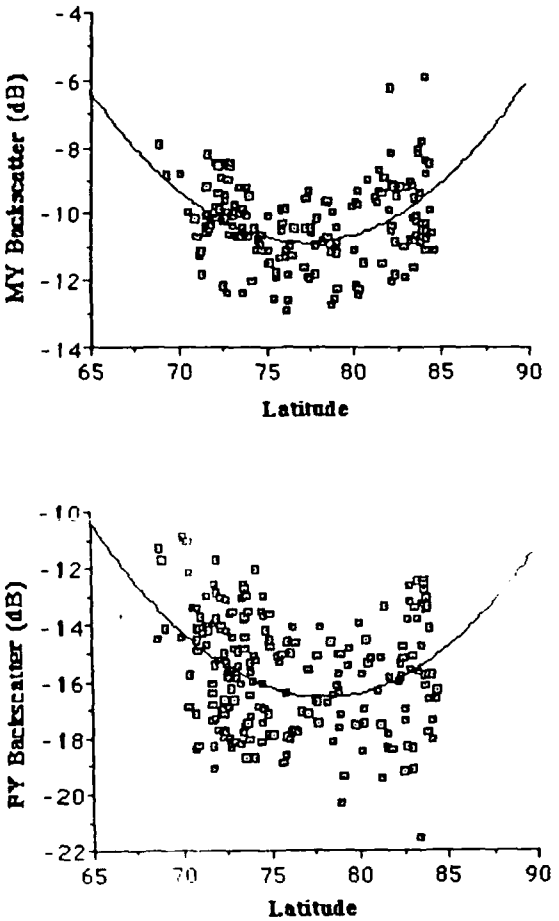

Figure 3. Backscatter of MY (top) and FY (bottom) ice as a function of latitude. Backscatter samples are drawn from the 60 images for which supervised classification was performed.

3. ICE MOTION

3.1 *Algorithm Evaluation*

The ice motion algorithm developed by JPL uses an area based cross-correlation and feature tracking method to produce motion vectors on a 5 km grid. Typically, two 100 km-square images separated in time by 3 days are submitted to the algorithm. The user selects the images to insure that some of the same floes or features are present in both. The algorithm makes use of filters to eliminate vectors with a low probability of being correct. In several of the image pairs evaluated, these filters were not successful in eliminating a few obviously erroneous vectors from about the image edges. The algorithm is fully described in Ref. 2.

To evaluate the algorithm, ice motion products were compared with ice motion vectors from an operational ice prediction model (the Polar Ice Prediction System or PIPS, Ref. 3.) and with vectors from satellite infrared data. Five pairs of SAR images were selected. Five corresponding pairs of satellite images from the Advanced Very High Resolution Radiometer (AVHRR) were submitted to a cross-correlation algorithm which produces vectors on a 10 km grid (Ref 4). The acquisition time for the SAR images led that of the AVHRR images by about 8 hours. Motion vectors from PIPS are available on a grid with spacing of about 45 km. PIPS vectors are 24-hour forecasts. Vectors from forecasts for the 3 days corresponding to the SAR motion pairs were averaged. The averages of all the vectors from PIPS, AVHRR, and SAR in the area covered by the SAR vectors are presented in Table 2.

Table 2. Ice motion from SAR compared with that from AVHRR and an operational model (PIPS). Motion direction was not obtained from PIPS. All image pairs or model runs are from dates in March, 1992.

Image pair dates	SAR (km/day)	SAR (direction)	AVHRR (km/day)	AVHRR (direction)	PIPS (km/day)
26,29	1.5	149°	1.2	169°	2.3
26,29	1.7	40°	0.2	50°	2.2
24,26	9.9	317°	4.0	312°	10.7
24,27	2.8	318°	1.7	315°	4.9
24,29	1.9	318°	0.4	270°	1.7

3.2 *Discussion*

The accuracy of motion vectors from satellite data depends on accurate geolocation of the satellite data, and on the accurate location of identical features in sequential imagery by an algorithm. Because SAR data are geolocated to within a few 100 meters, and because SAR combines high resolution with good discrimination of floes, the superior accuracy of motion vectors from SAR is not in question. In contrast, AVHRR images have a resolution which varies from about 1 km at nadir to about 4 km at swath edge. In the images used here, the coast of Alaska was often cloudy, which prevented checking the geolocation of the imagery with the coastline. In a larger AVHRR data set acquired for the Leadex experiment, AVHRR images had to be shifted an average of 4 km to match the coast. If the average error in AVHRR geolocation is taken as 4 km, this leads to a maximum ice velocity error of 3.8 km/day over a three-day period. Errors in AVHRR geolocation, therefore, can account for the differences in the magnitude of velocity between AVHRR and SAR vectors in Table 2.

The magnitude of velocity from the PIPS model is consistently greater than that from SAR. PIPS vectors depend to a large extent upon the input wind field. By providing a method of quantifying deformation and shear, SAR data can potentially modify this dependence.

4. CONCLUSIONS

The wintertime ice classification product is accurate to within about 10% when compared to the results of supervised classification using training sets. Much of the error is due to misclassification of a few images with unusually bright FY ice. Improved accuracy will come through better definition of the seasonal and regional domain of the algorithm. The small standard deviation of the algorithm when anomalous cases are excluded implies that algorithm accuracy can be improved by adjusting *a priori* ice type distributions.

The SAR motion product resolves shear and deformation missed by an operational model and coarser resolution satellite data. However, it is sometimes difficult to find image pairs for analysis, especially when ice is moving rapidly. The motion product will be most useful operationally when used to validate or update ice models, which show motion over a larger field.

5. REFERENCES

1. Kwok, R., E. Rignot, B. Holt, and R. Onstott 1992, Identification of sea ice types in spaceborne synthetic aperture radar data, *J. of Geophysical Research*, 97, C2, 2391-2402.

2. Kwok, R., J. C. Curlander, R. McConnell, and S. Pang 1990, An ice motion tracking system at the Alaska SAR Facility, *IEEE J. of Oceanic Engineering*, 15, 1, 44-54.

3. Preller, R. H. and P. G. Posey 1989, *The Polar Ice Prediction System - A Sea Ice Forecasting System*, Naval Ocean Research and Development Activity, Stennis Space Center, MS, NORDA Rpt. 212, 42pp.

4. Emery, W. J., C. W. Fowler, J. Hawkins, and R. H. Preller 1991, Fram Strait satellite image-derived ice motions, *J. of Geophysical Research*, 96, C3, 4751-4768.